PROCEEDINGS OF SCIENCE

Sensitivity of BEACON to Ultrahigh Energy Neutrinos

A. Zeolla,[a,*] **S. A. Wissel,**[a] **J. Alvarez-Muñiz,**[b] **W. Carvalho Jr.,**[c] **A. Cummings,**[a] **C. Deaconu,**[d] **K. Hughes,**[e] **R. Krebs,**[a] **Z. Martin,**[d] **K. Mulrey,**[f] **E. Oberla,**[d] **S. Prohira,**[g] **A. Romero-Wolf,**[h] **H. Schoorlemmer,**[i] **A. G. Vieregg**[d] **and E. Zas**[b]

[a] *Dept. of Physics, Penn State Univ., University Park, PA 16802*
[b] *Instituto Galego de Física de Altas Enerxías IGFAE,, Univerisade de Santiago de Compostela, 15782 Santiago de Compostela, Spain.*
[c] *Univerisade de São Paolo, Sao Pãolo, Brazil.*
[d] *Dept. of Physics, Enrico Fermi Inst., Kavli Inst. for Cosmological Physics, Univ. of Chicago, Chicago, IL 60637.*
[e] *Dept. of Physics, The Ohio State Univ., Columbus, OH 43210*
[f] *Physics Dept., Vrije Universiteit Brussel, Brussels, Belgium*
[g] *Dept. of Physics and Astronomy, Univ. of Kansas, Lawrence, KS 66045*
[h] *Jet Propulsion Laboratory, California Institute for Technology, Pasadena, CA 91109.*
[i] *Max-Planck-Institut für Kernphysik, Heidelberg, Germany*

E-mail: azeolla@psu.edu

The Beamforming Elevated Array for COsmic Neutrinos (BEACON) is a proposed detector concept consisting of many phased radio antenna arrays placed on mountaintops, searching for the upgoing extensive air showers created by Earth-skimming tau neutrinos. The high elevation sites and long propagation length of radio provide each station with a large detection area, while beamforming improves the signal-to-noise ratio and lowers the energy threshold. The stations are independent, and as such can be distributed globally. A Monte Carlo, which incorporates models of tau neutrino propagation, tau decay, and air shower radio emission, has been developed to predict the effective area of potential station layouts. Here, we give an overview of the BEACON concept, and present the predicted sensitivity of BEACON to ultrahigh energy transient and diffuse neutrino fluxes.

10th International Workshop on Acoustic and Radio EeV Neutrino Detection Activities (ARENA2024)
11-14 June 2024
The Kavli Institute for Cosmological Physics, Chicago, IL, USA

*Speaker

PoS(ARENA2024)039

1. Introduction

The sources of ultrahigh energy cosmic rays (UHECRs) remain unknown due to deflections by galactic magnetic fields. Ultrahigh energy neutrinos ($E > 100$ PeV), produced by interactions between photons and UHECRs near the sources, could potentially solve this problem since they travel unimpeded through space [1]. Additionally, these neutrinos have energies far exceeding what we can achieve with accelerators on Earth, allowing us to further probe fundamental particle physics [2]. Ultrahigh energy neutrinos remain undetected however, due to the extremely low flux at these energies. Next-generation neutrino detectors will need very large detector volumes in order detect an ultrahigh energy neutrino in a reasonable time-frame.

Astrophysical neutrinos are predicted to arrive at Earth with an equal flavor ratio, $\nu_e : \nu_\mu : \nu_\tau = 1 : 1 : 1$ [3]. Ultrahigh energy tau neutrinos present a unique opportunity for detection. As a tau neutrino skims the Earth, it can produce a tau lepton via a charged-current interaction. That tau lepton can then escape the Earth, and due to its short lifetime, decay shortly afterwards in the lower atmosphere. The decay initiates an up-going extensive air shower which emits radio coherently due to the separation of charged particles by Earth's magnetic field [4, 5]. Ultrahigh energy tau neutrinos could therefore be detected indirectly by observing the radio impulses created by these up-going extensive air showers.

The Beamforming Elevated Array for COsmic Neutrinos (BEACON) is a novel detector concept consisting of $O(1000)$ independent phased antenna arrays, placed on mountaintops, monitoring a vast area for these up-going, tau-induced extensive air showers [6]. From the mountaintops, each station can detect extensive air showers $O(100)$ km away due to the long propagation length of radio. Each station consists of $O(10)$ low-cost, short-dipole antennas with a phased array trigger, which enables a lower energy threshold and the directional rejection of noise. Since each station is independent, the stations can be distributed globally giving BEACON a large field-of-view. A prototype consisting of six crossed dipoles is currently deployed in the White Mountains of California near the Barcroft Field Station. The prototype is described in detail in [7].

In these proceedings, we calculate the predicted sensitivity of a full-size BEACON to both point-source and diffuse fluxes of UHE neutrinos. In section 2, we discuss the Monte Carlo used to perform this calculation, the simulation setup, and the results. In section 3, we show how including local topography in the Monte Carlo affects the predicted sensitivity of a single BEACON station. Lastly, we discuss the implications of these results in Section 4.

2. Monte Carlo and Results

A Monte Carlo was developed to numerically calculate the point source effective area of any arrangement of BEACON stations to tau neutrinos. The Monte Carlo, named the **M**ultiple **A**ntenna A**r**rays on **Mo**untains **T**au **S**imulation, or Marmots, accounts for potentially overlapping viewing areas between stations. Iterating over source positions in the sky, a cone extending from each station in the direction of the source is projected onto the Earth. The union of these projections is then found and uniformly populated with tau lepton exit points. The probability of each tau exiting the Earth, and the probability of each tau being subsequently detected given the station layout and design, is then calculated. Ultimately, Marmots outputs the instantaneous effective area

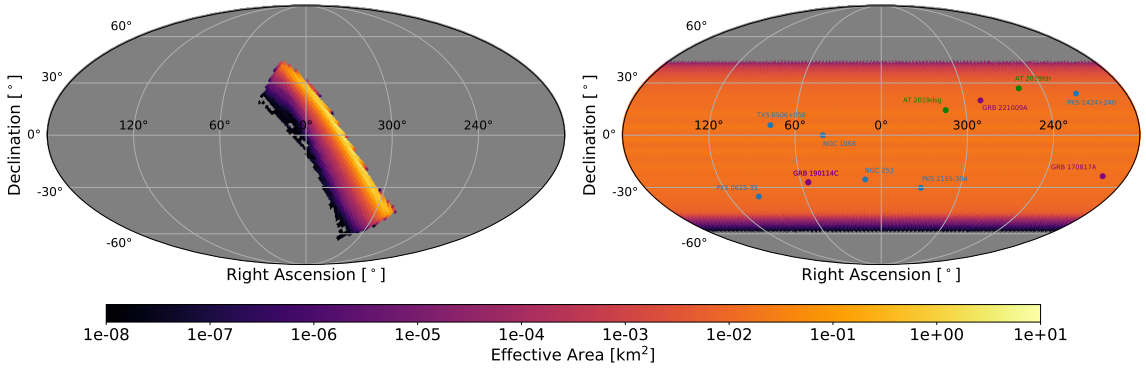

Figure 1: The instantaneous (left) and day-average (right) point-source effective area predicted by Marmots for a 100-station BEACON to 1 EeV tau neutrinos. Overlaid on the day-average effective area plot are the locations of various neutrino source candidates. In blue are AGN, blazars, and FSRQS, in green are tidal disruption events, and in purple are gamma ray bursts.

in each source direction (right ascension and declination) for the entire sky. Iteratively rotating and summing the instantaneous effective area over 360°, and then dividing by the total number of rotations, provides the day-averaged effective area. Marmots is described in greater detail in [8].

The BEACON concept consists of $O(1000)$ stations, each consisting of $O(10)$ antennas, at elevations greater than 2 km. Here, we simulate 100 stations, each containing 10 BEACON prototype antennas, elevated at 3 km above sea level. To estimate the effective area of 1000 stations we then scale the effective area result by a factor of 10. This estimation was done since simulating 1000 stations is computationally expensive. The stations are arranged along a line of equal longitude centered on the site of the BEACON prototype ($\lambda = 37.5893^\circ N$, $\phi = 118.2376^\circ W$) [7]. The stations are spaced 3 km apart in order to reduce the number of coincident events between them. The stations face East, where the geomagnetic effect is maximized, and have a field-of-view of 120°. Lastly, we assume a phased signal-to-noise ratio trigger threshold of 5 times thermal noise ($\sim 110\,\mu V$).

The effective area was calculated for tau neutrinos with energies ranging from 10^{16} to 10^{21} eV in half-decade bins. The instantaneous and day-average effective areas at 1 EeV are shown in Fig. 1. Overlaid on the day-average effective area plot are the locations of various neutrino source candidates. In blue are AGN, blazars, and FSRQS, in green are tidal disruption events, and in purple are gamma ray bursts.

The sensitivity of a detector to an all-flavor $dN_\nu/d\mathcal{E}_\nu \propto E_\nu^{-2}$ neutrino flux from point-sources is given by

$$E_\nu^2 \phi_\nu = \frac{2.44}{\ln(10)} \frac{3\,E_\nu}{A(E_\nu)}, \tag{1}$$

where $2.44/\ln(10)$ is the Feldman-Cousins factor for a 90% unified confidence level in which zero events were detected over a decade of energy [9], and the factor of 3 accounts for the fact that BEACON is sensitive to only one of three neutrino flavors.

The peak sensitivity of a 100-station BEACON to short-duration transients can be found by plugging the maximum instantaneous effective area at each energy into Eq. 1. This result is depicted by the solid black curve in Fig. 2. The dashed black curve shows the approximate sensitivity of a

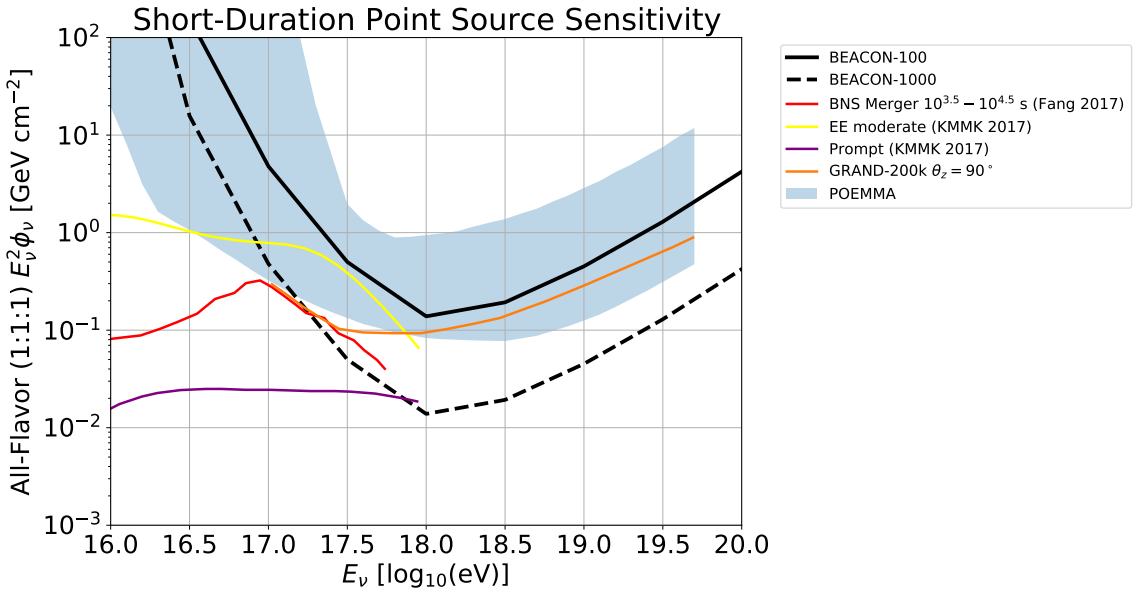

Figure 2: The sensitivity of a 100-station BEACON to short-duration point sources of neutrinos calculated using Eq. 1 and the maximum instantaneous effective area predicted by Marmots. Also shown is this sensitivity divided by a factor of 10, an approximation of the sensitivity of a 1000-station BEACON. These are compared to a model of the all-flavor fluence from a stable millisecond magnetar $10^{3.5}$ – $10^{4.5}$ s after a BNS merger, scaled to a source distance of 5 Mpc [10], and the modeled all-flavor fluence from sGRB viewed on-axis, scaled to a distance of 40 Mpc, during two phases: extended (EE) and prompt emission [11]. The short-duration point source sensitivity of the experiments GRAND-200k, at a zenith angle of 90° [12], and POEMMA [13] are also plotted.

1000-station BEACON, estimated by scaling the 100-station effective area by a factor of 10. These curves are compared to predicted neutrino fluences from BNS mergers at 5 Mpc [10], as well as from sGRB at 40 Mpc, viewed on-axis, during two phases: extended (EE) and prompt emission [11].

The sensitivity of a 100-station BEACON to long-duration transients can be found using Eq. 1 and the day-average effective area calculated by Marmots. The result is the solid gray band in Fig. 3. The band depicts the minimum and maximum sensitivity within the range of declinations $-40^\circ \leq \delta \leq 30^\circ$. Like before, the dashed band shows the same result scaled by a factor of 10 as an approximation for a 1000-station BEACON. Also plotted are the predicted neutrino fluences from BNS mergers to stable millisecond magnetars on two time scales, $10^{4.5}$ – $10^{5.5}$ s and $10^{5.5}$ – $10^{6.5}$ s, at a source distance of 5 Mpc [10].

Integrating the instantaneous or day-average effective areas over solid angle provides the acceptance $A\Omega(E_\nu)$. The sensitivity of a detector to an all-flavor $dN_\nu/d\mathcal{E}_\nu \propto E_\nu^{-2}$ diffuse neutrino flux is given by

$$E_\nu^2 \phi_\nu = \frac{2.44}{\ln(10)} \frac{3\, E_\nu}{A\Omega(E_\nu)\, T}, \tag{2}$$

where T is the exposure time. Shown in Fig. 4 is the 5-year diffuse flux sensitivity of a 100-station BEACON, as well as the scaled approximation for a 1000-station BEACON. These curves are compared to cosmogenic [14, 15] and astrophysical [16] diffuse neutrino flux predictions.

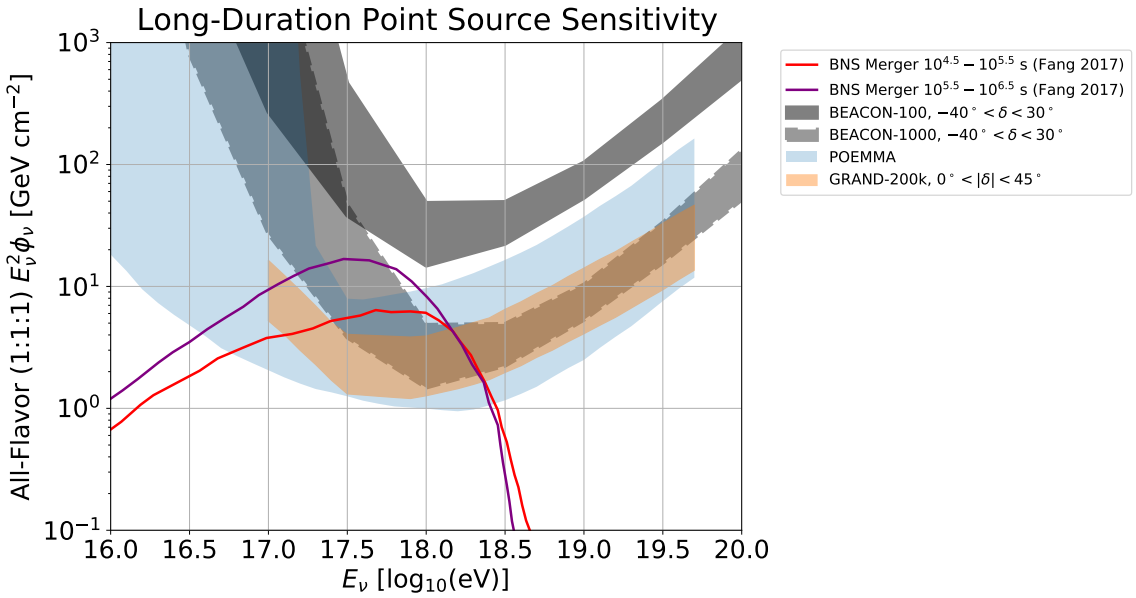

Figure 3: The sensitivity of a 100-station BEACON to long-duration transients calculated using Eq. 1 and the day-average effective area predicted by Marmots. The band depicts the minimum and maximum sensitivity within the range of declinations $-40° \leq \delta \leq 30°$. Also shown is this sensitivity divided by a factor of 10, an approximation of the sensitivity of a 1000-station BEACON. These are compared to the modeled all-flavor fluence from a stable millisecond magnetar $10^{4.5} - 10^{5.5}$ s and $10^{5.5} - 10^{6.5}$ s after a BNS merger, scaled to a source distance of 5 Mpc [10]. The sensitivity of the experiments GRAND-200k, over the declination range $0° < |\delta| < 45°$ [12], and POEMMA [13] are also plotted.

3. The Effect of Topography on Sensitivity

Up to now, these sensitivity estimates have assumed a perfectly smooth, spherical Earth. In reality, local topography will have an effect on the effective area of BEACON. Topography may improve the effective area by increasing the surface area being monitored or by providing additional targets for neutrino interactions, but it could also worsen the effective area by blocking line-of-sight to tau decays. It is difficult to tell what effect local topography may have without simulation.

Marmots was thus modified to account for topography. From each station, the position of the visual horizon in 0.25° bins is found within the field-of-view. We then extend beyond this distance by 100 km to account for the fact that taus can pass through terrain before decaying. The union of these areas is found and then triangulated. At the latitude and longitude of each triangle vertex the elevation is found via the SRTM database [17]. In this way, a 3D triangle mesh of the Earth's surface is generated. For each point source, we then filter out the triangles outside the view-angle cone. Those that remain have tau exit points uniformly sampled over their surfaces.

From each exit point, the grammage of Earth traversed by the tau neutrino is calculated. This is done by finding all backwards intersections with the 3D triangle mesh. The grammage of steeply up-going tau neutrinos is calculated assuming a spherical Earth. From the grammage we can then determine the probability that the tau exits the Earth, as well as its energy. Line-of-sight between tau decays and each station is then checked by searching for intersections with the 3D triangle

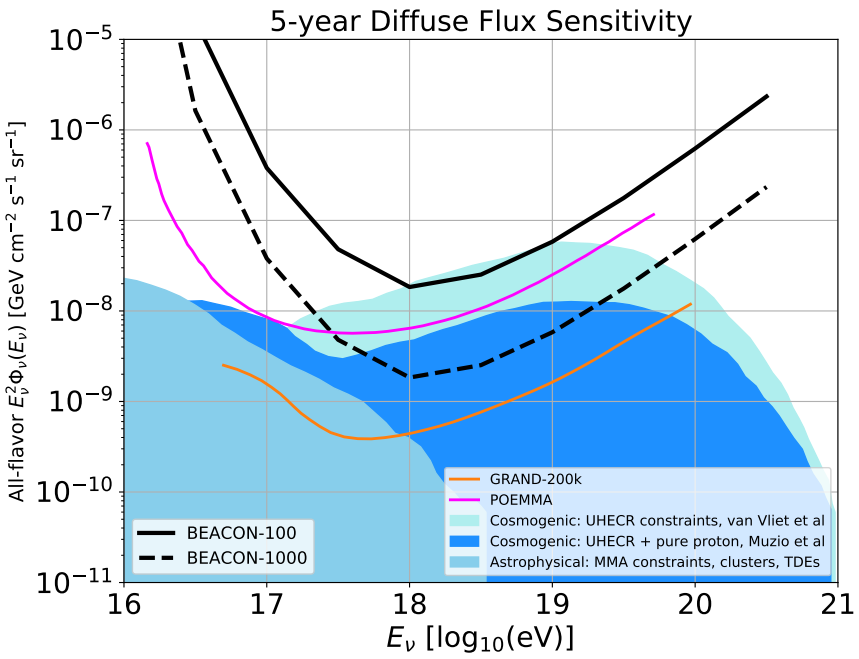

Figure 4: The 5-year diffuse flux sensitivity of a 100-station BEACON calculated using Eq. 2. Also shown is this sensitivity divided by a factor of 10, an approximation of the sensitivity of a 1000-station BEACON. These curves are compared to cosmogenic [14, 15] and astrophysical [16] diffuse neutrino flux predictions. The diffuse flux sensitivity of the experiments GRAND-200k [12], and POEMMA [13] are also plotted.

mesh. If line-of-sight to a decay is blocked for all stations, then the resulting shower is considered undetectable.

The aperture of a single 10-antenna station located at the BEACON prototype site (λ = 37.5893° N, ϕ = 118.2376° W, h = 3.85 km) was calculated for both a smooth Earth and one with local topography. The results are shown in Fig. 5. At all energies the aperture is increased by including topography, however the magnitude of the effect is energy dependent.

4. Conclusions

Combining the large field-of-view of BEACON with a position near the equator provides the experiment with excellent sky coverage over the course of a day, as seen in Fig. 1. With 5 years of exposure, 100-stations of BEACON can begin to probe cosmogenic flux models, as seen in Fig. 4. The design particularly excels in its instantaneous effective area however, thanks to the high altitude observation sites. With just 100 stations, BEACON has a sensitivity to short-duration transients comparable to GRAND and POEMMA. With 1,000 stations, BEACON is sensitive to short-duration transients such as BNS mergers and sGRBs, as seen in Fig. 2. BEACON is a highly efficient design, incorporating only 1,000 short-dipole antennas in a 100-station design, and 10,000 antennas in a 1000-station design. Initial results with Marmots, modified to include topography, suggests that topography can further enhance the predicted sensitivity by up to a factor of 3. The

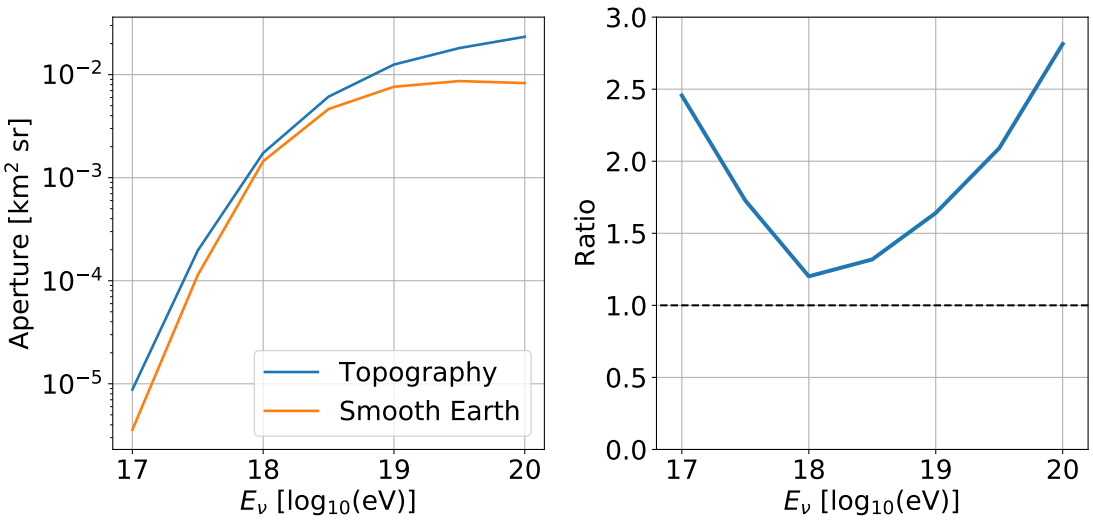

Figure 5: Left: the aperture single BEACON station located the prototype site ($\lambda = 37.5893° N$, $\phi = 118.2376° W$, $h = 3.85$ km) with and without topography enabled in Marmots. Right: the ratio of the "Topography" result to the "Smooth Earth" result.

effect of topography on sensitivity will be site dependent, making Marmots a valuable tool for site selection.

This work is supported by NSF Awards # 2033500, 1752922, 1607555, PHY-2012980, and DGE-1746045 as well as the Sloan Foundation, the RSCA, the Bill and Linda Frost Fund at the California Polytechnic State University, and NASA (support through JPL and Caltech as well as Award # 80NSSC18K0231). This work is also funded by Xunta de Galicia (CIGUS Network of Res. Centers & Consolidación ED431C-2021/22 and ED431F-2022/15), MCIN/AEI PID2019-105544GB-I00 - Spain, and European Union ERDF. We thank the NSF-funded White Mountain Research Station for their support. Computing resources were provided by the University of Chicago Research Computing Center.

References

[1] M. Ackermann et al., *Astrophysics Uniquely Enabled by Observations of High-Energy Cosmic Neutrinos*, *Bull. Am. Astron. Soc.* **51** (2019) 185 [1903.04334].

[2] M. Ackermann et al., *Fundamental Physics with High-Energy Cosmic Neutrinos*, *Bull. Am. Astron. Soc.* **51** (2019) 215 [1903.04333].

[3] J.F. Beacom, N.F. Bell, D. Hooper, S. Pakvasa and T.J. Weiler, *Measuring flavor ratios of high-energy astrophysical neutrinos*, *Phys. Rev. D* **68** (2003) 093005.

[4] E. Zas, *Neutrino detection with inclined air showers*, *New Journal of Physics* **7** (2005) 130.

[5] F.G. Schröder, *Radio detection of cosmic-ray air showers and high-energy neutrinos*, *Progress in Particle and Nuclear Physics* **93** (2017) 1–68.

[6] S. Wissel et al., *Prospects for high-elevation radio detection of >100 PeV tau neutrinos*, *JCAP* **11** (2020) 065 [2004.12718].

[7] D. Southall et al., *Design and Initial Performance of the Prototype for the BEACON Instrument for Detection of Ultrahigh Energy Particles*, *NIM-A* **1048** (2023) 167889 [2206.09660].

[8] A. Zeolla et al., *Sensitivity of BEACON to Point Sources of Ultrahigh Energy Neutrinos*, *PoS* **ICRC2023** (2023) 1020.

[9] G.J. Feldman and R.D. Cousins, *A Unified approach to the classical statistical analysis of small signals*, *Phys. Rev. D* **57** (1998) 3873 [physics/9711021].

[10] K. Fang and B.D. Metzger, *High-Energy Neutrinos from Millisecond Magnetars formed from the Merger of Binary Neutron Stars*, *Astrophys. J.* **849** (2017) 153 [1707.04263].

[11] S.S. Kimura, K. Murase, P. Mészáros and K. Kiuchi, *High-Energy Neutrino Emission from Short Gamma-Ray Bursts: Prospects for Coincident Detection with Gravitational Waves*, *Astrophys. J. Lett.* **848** (2017) L4 [1708.07075].

[12] GRAND collaboration, *The Giant Radio Array for Neutrino Detection (GRAND) project*, *PoS* **ICRC2021** (2021) 1181 [2108.00032].

[13] T.M. Venters, M.H. Reno, J.F. Krizmanic, L.A. Anchordoqui, C. Guépin and A.V. Olinto, *POEMMA's Target of Opportunity Sensitivity to Cosmic Neutrino Transient Sources*, *Phys. Rev. D* **102** (2020) 123013 [1906.07209].

[14] A. van Vliet, R. Alves Batista and J.R. Hörandel, *Determining the fraction of cosmic-ray protons at ultrahigh energies with cosmogenic neutrinos*, *Phys. Rev. D* **100** (2019) 021302 [1901.01899].

[15] M.S. Muzio, G.R. Farrar and M. Unger, *Probing the environments surrounding ultrahigh energy cosmic ray accelerators and their implications for astrophysical neutrinos*, *Phys. Rev. D* **105** (2022) 023022 [2108.05512].

[16] M. Ackermann et al., *High-energy and ultra-high-energy neutrinos: A Snowmass white paper*, *JHEAp* **36** (2022) 55 [2203.08096].

[17] T.G. Farr et al., *The Shuttle Radar Topography Mission*, *Reviews of Geophysics* **45** (2007) RG2004.

PoS(ARENA2024)039